

ANATOMIC AND MORPHOLOGIC DESCRIPTION OF THE RENAL PELVIS OF THE
HORSE USING MAGNETIC RESONANCE IMAGING OF POLYMER CASTS,
URETEROPYELOSOPY, AND HISTOLOGY

By

Santiago Garcia Pasquel

A THESIS

Submitted to
Michigan State University
in partial fulfillment of the requirements
for the degree of

MASTER OF SCIENCE

Large Animal Clinical Sciences

2012

ABSTRACT

ANATOMIC AND MORPHOLOGIC DESCRIPTION OF THE RENAL PELVIS OF THE HORSE USING MAGNETIC RESONANCE IMAGING OF POLYMER CASTS, URETEROPYELOSCOPY, AND HISTOLOGY

By

Santiago Garcia Pasquel

Descriptions of the equine renal pelvis in textbooks are inconsistent and unsuitable for guiding ureteropyeloscopy. To document the anatomy of the upper urinary collecting system of the horse, specifically the renal pelvis, kidneys were harvested from 10 horses and magnetic resonance imaging was performed after distension of the renal pelvis with a polymer cast material. Transurethral ureteropyeloscopy of the upper urinary tract was also performed in four horses and followed by histological and immunohistochemical examination of the renal medulla and pelvis. The equine renal pelvis was found to be a funnel-shaped cavity, flattened dorsoventrally in the craniocaudal direction. Multiple inner medullary collecting ducts (IMCDs) from the central part of the kidney open along an ~3 cm long renal crest that protrudes into the renal pelvis while IMCDs from each pole open into two long (6-7 cm), narrow *tubi maximi* that terminate at either end of the renal crest. The diameter of the distended *tubi maximi* are narrowest (~3 mm) at their junction with the renal crest. Openings of the *tubi maximi* could be visualized during ureteropyeloscopy in all horses and minor anatomical variation was observed. Histological examination and immunohistochemical staining for smooth muscle actin demonstrated increased amounts in a band pattern in the outer medullary region as well as at the junction of the *tubi maximi* with the renal crest. This study found that currently available endoscopic equipment can be used to visualize the renal pelvis and renal crest but cannot be advanced into the *tubi maximi*.

TO MY PARENTS, MENTORS, COLLEAGUES AND ALL THE HORSES THAT HELPED
ME ACHIEVE THIS RESEARCH.

TABLE OF CONTENTS

LIST OF TABLES.....	vi
LIST OF FIGURES.....	vii
KEY TO SYMBOLS AND ABBREVIATIONS.....	ix
CHAPTER 1: INTRODUCTION.....	1
ENDOSCOPY OF THE URINARY TRACT.....	1
EQUIPMENT MOST COMMONLY USED DURING FLEXILE URETEROSCOPY.....	2
GUIDE WIRES.....	2
ACCESS SHEATHS.....	2
FLEXIBLE ENDOSCOPES.....	3
INTRACORPOREAL LASER ELEMENTS.....	3
ENDOSCOPY OF THE UPPER URINARY TRACT IN HUMANS.....	3
ANATOMY OF THE EQUINE KIDNEYS.....	4
RIGHT KIDNEY.....	5
LEFT KIDNEY.....	5
WEIGHT.....	6
STRUCTURE.....	6
RENAL CAPSULE.....	6
CORTEX AND MEDULLA.....	7
BLOOD SUPPLY.....	8
SMOOTH MUSCLE IN THE RENAL MEDULLA.....	10
RENAL PELVIS.....	10
BIBLIOGRAPHY.....	15
CHAPTER 2: ANATOMIC AND MORPHOLOGIC DESCRIPTION OF THE RENAL PELVIS OF THE HORSE USING MAGNETIC RESONANCE IMAGING OF POLYMER CASTS, URETEROPYELOSOCOPY, AND HISTOLOGY.....	20
REASONS FOR PERFORMING STUDY.....	20
OBJECTIVE:.....	20
METHODS:.....	20
RESULTS:.....	20
CONCLUSIONS:.....	21
POTENTIAL RELEVANCE:.....	21
INTRODUCTION.....	21
MATERIALS AND METHODS.....	23
RESULTS.....	32
DISCUSSION.....	42

CONCLUSION.....	45
BIBLIOGRAPHY	46

LIST OF TABLES

Table 1: Mean \pm S.D. values (range) for kidney weight, kidney length measured at necropsy, kidney length measured via MRI, kidney volume measured by water displacement, and kidney volume measured by MRI in 10 horses. Table 1. Mean \pm S.D. values (range) for kidney weight, kidney length measured at necropsy, kidney length measured via MRI, kidney volume measured by water displacement, and kidney volume measured by MRI in 10 horses..... 33

Table 2: Mean \pm SD values (range) for MRI measurements of renal crest length, renal crest volume, diameter of the renal pelvis, length of the cranial and caudal tubi maximi, and diameter of the cranial and caudal tubi maximi at their origin (pole end), midpoint, and termination (pelvis end) in 10 horses. 35

LIST OF FIGURES

Figure 1: Dorsal plane photographs (top) and magnetic resonance images (bottom) of the left (A) and right (B) kidneys showing (lines) where kidney length was measured. “For interpretation of the references to color in this and all other figures, the reader is referred to the electronic version of this thesis”..... 26

Figure 2: Three dimensional reconstruction of polymer within a left kidney detailing where measurements were made: 1. length of the cranial tubus maximus; 2. length of caudal tubus maximus; 3. renal crest length; 4. renal pelvis proximal diameter; 5. renal pelvis middle diameter; 6. renal pelvis distal diameter; 7. diameter of the pelvic end of the cranial tubus maximus 8. diameter of the midpoint of the cranial tubus maximus; 9. diameter of the pole end of the cranial tubus maximus; 10. diameter of the pelvic end of the caudal tubus maximus 11. diameter of the midpoint of the caudal tubus maximus; and 12. diameter of the pole end of the cranial tubus maximus. “For interpretation of the references to color in this and all other figures, the reader is referred to the electronic version of this thesis”..... 27

Figure 3: Diagram of a left kidney showing the pattern used to section the kidney for subgross anatomical and histopathological examination..... 30

Figure 4: Corrosion polymer cast of the renal pelvis: top panel shows a tubus maximus (a) extending from the renal pelvis (b) with polymer extending into numerous papillary ducts (c) along its length; bottom panel shows the narrowing of the tubus maximus at its junction with the renal pelvis (arrow) “For interpretation of the references to color in this and all other figures, the reader is referred to the electronic version of this thesis”..... 36

Figure 5: Ureteropyeloscopic images of the renal pelvis before (A-C) and after (D-F) intravenous administration of phenol red (orientation - cranial to the left, bubbles are dorsal): A. appearance of the renal crest (1) surrounded by uroepithelium (2) at the proximal aspect of the ureter (3); B. closer view of the entire renal crest within the renal pelvis showing fornices (2) above and below the renal crest and openings of the tubi maximi (4) towards either end of the renal crest; C. anatomic variation of the renal pelvis with a recess in the center (5) into which several papillary ducts open; D. cranial aspect of the renal crest showing urine discolored by phenol red entering the renal pelvis from the cranial tubus maximus (4); E. caudal aspect of the renal crest showing urine discolored by phenol red entering the renal pelvis from the caudal tubus maximus (4); and F. central portion of the renal crest showing urine discolored by phenol red exiting numerous papillary ducts. “For interpretation of the references to color in this and all other figures, the reader is referred to the electronic version of this thesis”..... 38

Figure 6: Panels A-C: pictures of subgross sagittal sections of a left kidney (fixed by distension of the renal pelvis with 10% formalin) showing the cortex (1), outer medulla (2), and inner medulla and tubus maximus (3) at the cranial pole end (A, section 2, see Figure 3 for section locations), the midpoint (B, section 4), and near the pelvis (C, section 6); panels D-F: pictures of subgross sagittal sections (section 6 or 10) of kidneys of three horses near the junction of the tubus maximus with the renal pelvis, also showing uroepithelium at the origin of the ureter. “For interpretation of the references to color in this and all other figures, the reader is referred to the electronic version of this thesis” 39

Figure 7: Subgross anatomic photographs (column 2) and low (2x, columns 3 & 4) and high power (100x, columns 5 & 6) photomicrographs stained with hematoxylin and eosin (columns 3 & 5) and immunolabeled for smooth muscle actin (SMA, columns 4 & 6). The numbers in column 1 refer to the kidney sections illustrated in Figure 3 and the small dash-lined boxes in columns 2 & 3 show the areas enlarged in columns 3 & 4 and 5 & 6, respectively. Note the more intense SMA immunolabeling towards the periphery in panel E and the upper right of panel F as well as surrounding the mid-portion of the tubus maximus (panel F) and, even more intensely, around the tubus maximus as it enters the renal pelvis (panel G). Intense SMA immunolabeling was also detected surrounding the papillary ducts as they terminated on the renal crest (panel H). The higher magnification photomicrographs reveal patchy SMA immunolabeling in the connecting tissue adjacent to most uroepithelial surfaces. “For interpretation of the references to color in this and all other figures, the reader is referred to the electronic version of this thesis”. 40

Figure 8: Photomicrographs of a sagittal section (section 4 in Figure 3) stained with hematoxylin and eosin (lower panel) and for smooth muscle actin (SMA, upper panel). Note the more intense aggregates of SMA immunolabeling in the outer portion of the inner medulla (between a and b), along a column extending into the deepest portion of the medulla (below c), as well as around the tubus maximus (the more diffuse dark band running from top to bottom to the right of c is an artifact). “For interpretation of the references to color in this and all other figures, the reader is referred to the electronic version of this thesis” 41

KEY TO SYMBOLS AND ABBREVIATIONS

IMCDs	Inner medullary collecting ducts
SMA	Smooth muscle actin

CHAPTER 1: INTRODUCTION

The purpose of this study was to describe the internal anatomy of the urinary tract, specifically the renal pelvis, of the horse in order to facilitate future endoscopic diagnostic and therapeutic procedures. Variability in renal pelvic anatomy between species, as well as inconsistent anatomic descriptions of the equine renal pelvis in veterinary textbooks, made use of currently available information unsuitable for the goals of the author and was the impetus for this research.

ENDOSCOPY OF THE URINARY TRACT

Over the past 40 years technological advances have guided medicine away from a more invasive approach including open surgical biopsies and organ extractions to less invasive procedures utilizing laparoscopy and natural orifice endoscopy for diagnostic and therapeutic procedures [1-3]. In the horse urethroscopy and cystoscopy have been performed since the mid-1970s to directly visualize disorders of the lower urinary tract, including urethroliths and cystoliths, neoplasms, and urethral defects and strictures [4-6]. However, evaluation of upper urinary tract disorders has largely been accomplished using imaging techniques including radiography, ultrasonography, and nuclear scintigraphy [7-9]. Disorders including ectopic ureter, nephrolithiasis, and renal neoplasia are examples of upper tract diseases that may be diagnosed using these imaging modalities [10, 11]

In human medicine, endoscopy of the upper urinary tract (ureterorenoscopy) has been successfully used for diagnostic evaluation and treatment of upper urinary tract disorders over the past couple of decades [12]. Recent development of smaller diameter, flexible, high resolution endoscopic equipment has also opened the potential for direct visualization of the ureter and renal pelvis of the horse.

EQUIPMENT MOST COMMONLY USED DURING FLEXILE URETEROSCOPY

With the exponential evolution in instrumentation and ever growing array of tools and technology available to endurologists, ureteropyeloscopy has grown as a diagnostic and therapeutic option for several pathologies. The diversity of tools available make it a topic of its own: for that reason the current chapter aims at describing the major aspects of the most common tools used in this branch of endoscopy.

GUIDE WIRES

Guidewires are wires of different diameters made of stainless steel designed to be introduced into narrow or irregular lumens prior to introduction of an endoscope. Advancement of a flexible endoscope is better achieved when it is introduced over a more rigid structure such a wire. Guidewires are made in several configurations (monofilament, coiled), different lengths, diameters, tip configurations, flexibility and coating among other properties, each designed for a specific purpose [13]. The ideal wire requires flexibility to respond to resistance encountered along the path, rigidity to allow safe and accurate passage of the endoscope, and lubrication on the surface to reduce friction. [14]

ACCESS SHEATHS

Access sheaths are synthetic sleeves that facilitate introduction of endoscopic instruments (endoscopes, wires, biopsy instruments, etc.) into urinary orifices while decreasing forces created on the stoma or opening. [15] Access sheaths have been associated with less postoperative complications, ease of reentry during the procedure, and improved outcome of intrarenal ureteroscopic surgery. [16] Another important characteristic of access

sheaths is their ability to maintain low intrapelvic pressures when highly pressurized irrigation is used. [17]

FLEXIBLE ENDOSCOPES

Endoscopes are made in a variety of diameters, lengths, materials, and flexibility. An endoscope to be used in ureteroscopy should provide adequate resolution, flexibility, and imaging capabilities to allow access and visualization of all of the internal structures of the collecting system of the kidney. [14] Most endoscopic equipment also has a biopsy port or intraluminal channel that allows irrigation and introduction of guide wires, biopsy instruments, and laser fibers.

INTRACORPOREAL LASER ELEMENTS

Once any abnormalities (areas of hemorrhage, etc.) or foreign elements (calculi) are visualized using the endoscope, intracorporeal elements such as lasers or electrohydraulic lithotriptors can be used for ablation or lithotripsy. Currently, use of Holium lasers has higher efficacy at fragmenting all compositions of urinary calculi and has been proven to reduce the need for secondary procedures.[18-21]

ENDOSCOPY OF THE UPPER URINARY TRACT IN HUMANS

The most common protocol used for human patients in whom the upper urinary tract needs to be visualized is as follows. The patient is first sedated and once sedation or anesthesia is adequate the procedure is started by passing a small caliber (6-7 F) flexible endoscope transurethrally into the bladder. The bladder is examined in its entirety along with the ureteral orifices to detect any pathologies present or anatomical variations. A guide wire is subsequently advanced into the ureter via the biopsy channel of the endoscope to facilitate passage of the endoscope into the

ureter. In some instances where the introduction is difficult the use of endoscopic access sheaths prior to introduction of the endoscope facilitates ureteral entry[14]. Once the endoscope is located into the ureter the guide wire is retracted into the biopsy channel. [22]

The ureter is examined as the endoscope is slowly passed up the ureter to the renal pelvis. Once in the renal pelvis, systematic examination of the upper, middle and lower major calyces is performed. Systematic examination limits the risk of confusion due to endoscopic bruising of the upper pole infundibulum. Bruising is most commonly caused by passive deflection of the endoscope against the upper pole area during inspection of the middle and lower pole calyces. Contrast medium can also be injected under fluoroscopic guidance to verify entry into all calices of the renal collecting system. [22] If a lesion is identified, the location needs to be carefully documented. As can be inferred, knowledge of the anatomy of the ureter and renal pelvis, as well as the range of anatomic variation, is essential for successful completion of upper urinary tract endoscopic procedure.

ANATOMY OF THE EQUINE KIDNEYS

The kidneys are two parenchymatous organs located in the abdominal cavity; each one is located under the psoas muscle group located under either side of the lumbar region of the vertebral column. The kidneys are maintained in their position in the abdomen by support from three structures: 1) an envelope of cellulo-adipose tissue; 2) the peritoneum which passes beneath them; and 3) the presence of the digestive organs in the abdominal cavity [23]. Externally, the kidneys resemble a bean or the heart of a playing card. The latter description is most appropriate for the equine right kidney while the left equine kidney is more commonly bean-shaped, and

sometimes elongated. Each kidney has two surfaces (dorsal and ventral), two borders (medial and lateral) and two extremities or poles (cranial and caudal).

RIGHT KIDNEY

The right kidney is located more cranially than the left kidney and extends forward beneath the last two ribs [23]. The cranial pole of the right kidney is embedded in the renal fossa of the liver. The dorsal surface of the right kidney is convex and makes contact craniodorsally with the diaphragm and caudodorsally with the great psoas muscle and the iliac fascia. The ventral surface is concave and is in contact with the pancreas, suprarenal capsule, and base of the cecum by loose connective tissue. The medial border is also convex and in contact with the caudal vena cava and psoas muscle. There is a deep notch in the center of the medial border termed the *renal hilus*, which leads into the *renal sinus*. The renal artery and nerves enter while the ureter and renal vein exit the kidney through the renal hilus; the renal sinus contains the renal pelvis or dilated proximal portion of the ureter. The lateral border is rounded and thinner in height than the medial border. It consists of cranial and caudal parts that meet at a lateral angle: the cranial part fits into the renal impression in the liver and the duodenum curves around the lateral border as it travels caudally. The caudal pole is thinner and narrower than the cranial pole.

LEFT KIDNEY

The left kidney is situated in a similar but more caudal location in the retroperitoneal space below or behind the last rib. The left kidney can be longer and narrower than the right kidney. The dorsal surface is convex and extends to the left crus of the diaphragm and is bordered by the iliac fascia and psoas muscles and the dorsal margin of the spleen. The ventral surface is convex and overlays the small colon, terminal duodenum, left adrenal gland, and the left extremity of the pancreas [24]. The medial border is longer, straighter and thicker than that of the right kidney

and is adjacent to the abdominal aorta, adrenal gland, and ureter. The lateral border extends to the dorsal aspect of the spleen. The cranial extent reaches the *saccus cecus* of the stomach, near the left side of the pancreas and the splenic vessels. There is a ligament attaching the spleen and the left kidney called the nephrosplenic (renosplenic) ligament. The shape of the left kidney is more variable than that of the right kidney, in some instances it is similar to the right kidney while in other horses, it may be more elongated and bean or J-shaped.

WEIGHT

One commonly used veterinary textbook provides an average weight of the equine right kidney of 765 g, a value that is greater than an average weight of the left kidney of 708 g [23, 24]. In a recent review, the right kidney was described to be 650 g and the left kidney 600 g with a total renal weight to body weight ratio of 1:300-350 [25]. However, the reverse relation has been reported (left kidney heavier than the right) as well as kidneys that are similar in weight [24].

STRUCTURE

RENAL CAPSULE

The surface of the kidney is covered by a thin, strong fibrous capsule that is continued into the renal sinus [24]. This fibrous membrane is intimately attached to the underlying renal parenchyma and envelopes the vessels, nerves, and ureter as they enter or exit the renal sinus [23]. The renal capsule consists of two layers: 1) an outer connective tissue layer composed of collagen and scattered elastic fibers; and 2) an inner layer composed of loose collagenous and reticular fibers along with a few smooth muscle cells [26]. The reticular fibers of the inner layer penetrate into the parenchyma of the kidney [26].

CORTEX AND MEDULLA

Kidneys are comprised of an outer cortex and an inner medulla. The cortex is red-to-brown in color, has a granular appearance on cut section, and it is dotted with minute dark points termed renal corpuscles (*Malpighian corpuscles*). Each corpuscle is formed by a dilated origin of a renal tubule (*capsula glomeruli* or *Bowman's capsule*) enclosing an invaginated tuft of capillaries (glomerulus). The medulla is wider than the cortex and shows radial striation on cut section, with pale deep central zones bordered by an undulating intermediate (corticomedullary) zone of deep red color. Interlobar arteries are regularly spaced in this intermediate zone. Between the vessels the medulla extends outward somewhat further toward the cortex, forming bases of structural units of the medulla, termed *renal pyramids*. In theory, each renal pyramid is associated with an overlying lobe of renal cortical tissue with all the nephrons in that lobe emptying urine via collecting ducts that travel through its papilla, the apex or innermost part of the pyramid adjacent to the renal pelvis. In some species, these individual structural and functional units within the kidney are clearly separated by invaginations of renal cortical tissue, termed *renal columns* (*columns of Bertin*).

The degree of separation produced by renal columns varies widely between species with some (cow, bear, otter, seal, and porpoise) having renal columns that completely surround the medullary tissue to the point that each subunit is essentially a separate kidney [20]. This type of morphology is termed a *rencular kidney* and external lobation is visually apparent. In contrast, at the other end of the spectrum, species such as the horse, dog, and cat have poorly developed renal columns such that cortical lobes and medullary pyramids are largely fused and kidneys appear to be unilobar on external appearance [14]. Two of the most widely studied veterinary anatomy textbooks describe equine kidneys to have 40-60 pyramids that are arranged in four

rows with the central ones being more distinct [24] and that equine kidneys are composed of 40-64 lobes that have completely fused [27]. Although the number of lobes and pyramids are similar, the degree of separation (or lack thereof) is not well described in available textbooks.

The marked species heterogeneity in gross and subgross renal anatomy has led to attempts to explain these differences along phylogenetic lines. However, these efforts have not been highly successful raising the suggestion that both divergence and convergence have played evolutionary roles in the similarity and dissimilarity of renal morphology between species [20].

BLOOD SUPPLY

At rest equine kidneys receive 20-25% of cardiac output [25, 28]. The kidney is considered a highly efficient organ; it possesses a highly specialized vascular arrangement to efficiently promote filtration in different biological status.

The main vascular configuration of the kidney is preserved across species [29]. Blood enters the kidneys through one or more renal arteries that branch from the aorta and enter the renal hilus through the ventral aspect of the kidney. Renal arteries divide into interlobar arteries that cross the renal medulla and in some species they are located in the columns of Bertini (cortical extensions that divide the medulla). The interlobar arteries branch into anastomotic arches (arcuate arteries) located at the corticomedullary junction. [23, 24]. Branches of the arcuate arteries called interlobular arteries pass into the cortex along a radial course between cortical lobules and give off short afferent arterioles that enter renal corpuscles to form the glomerular capillaries. Blood exits the glomeruli to form the efferent arteriole that divides into a series of peritubular capillaries around the remainder of the nephron. The network of peritubular capillaries around the cortical portion of the nephron is more extensive, to accommodate

reabsorption of a large portion of glomerular filtrate, than in the inner medulla where the peritubular capillaries, termed vasa recta, become aligned with the limbs of the loop of Henle.

The vascular structure of the renal medulla is complex and in order to better explain it, is necessary to divide it into an outer and inner medulla. The outer medulla is further subdivided into the outer stripe which is in contact with the renal cortex, and an inner stripe that contacts the inner medulla. [30] The outer stripe is formed by many descending vasa recta that originate from the efferent arterioles of the glomeruli. The inner stripe of the outer medulla is composed by separate conglomerates or bundles of vasa recta that have two branches, one will eventually penetrate to the inner medulla and another that will give rise to a separated vascular plexus. The latter vascular plexus provides the blood supply to the highly metabolic thick ascending limb of Henle's loop.[30]

The difference between the bundles and the plexi of the inner stripe gives rise to the speculation that constriction of the bundle should increase the perfusion of the plexus (interbundle area) and this notion is supported by evidence that blood flow to the renal medulla can be altered independently from cortical blood flow. [31]

The descending vasa recta in the bundle continue their descent into the inner medulla where they become fenestrated and give rise to ascending vasa recta. The ascending vasa recta are also located within bundles. The apposition of descending and ascending vasa recta allows equilibration water and solute within the interstitium surrounding the loops of Henle. [30] The ascending branches of vasa recta drain into venules that lead to interlobar veins. In the superficial part of the cortex, small veins converge into star-shaped venous structures, termed *venulae stellatae*, that drain into renal veins. Renal veins are large and thinned walled, again to

accommodate return of large volumes of filtered fluid to the circulation, and drain into the caudal vena cava.

SMOOTH MUSCLE IN THE RENAL MEDULLA

The descending vasa recta are in structure similar to capillaries as they lack a smooth muscle layer. However, they are partly surrounded by cells with contractile elements termed pericytes that persist into the inner medulla but eventually disappear.[32] Pericytes contain α -smooth muscle actin and it is speculated that they have contractile properties that could regulate blood flow distribution within the medulla.[33] As an example, Franchini and Cowley (1996) showed that inner medullary blood flow was reduced without a change in outer medullary blood flow after 48 hours of water restriction in rats and attributed this differential response to pericyte action [34]

RENAL PELVIS

The papillae of the kidneys secrete urine into a cavity called the “renal pelvis”. The renal pelvis can also be considered to be the dilated origin of the ureter that lies in the renal sinus. Histologically, the renal pelvis consists of three layers: 1) an external fibrous coat or adventitia; 2) an intermediate smooth muscle layer; and 3) an innermost layer of transitional epithelium that is also rich in tubular glands that secrete viscid mucus into the renal pelvis. Smooth muscle fibers in the middle layer run in assorted directions, attaching near the site where the fibrous coat of pelvis attaches to the papillae, and continuing without interruption as ureteral smooth muscle [35]. The inner transitional epithelial layer can form several folds and has a yellowish color [35].

Although there has been considerable investigation and description of species variation in parenchymal morphology of mammalian kidneys during the past century, until more recently, less attention had been paid to variation in renal pelvic anatomy

Preparation of casts comprised of various materials has been a common method used by anatomists to examine and describe cavitory anatomical structures. For example, Leonardo da Vinci (1452 – 1519) studied casts made of molten wax to better understand and illustrate the ventricles of the brain [36] and since that time use of corrosion casts has furthered understanding of anatomical structures in a way that dissection alone would not permit.

The renal pelvis has been investigated by use of cast material because, as eloquently stated in 1951 by Naranth, “hardly any organ in the *Mammalia* exhibits such variation in form as the renal pelvis” [37]. Further, discernible phylogenetic patterns of renal pelvic morphology appear to be lacking as the anatomy of the renal pelvis may vary considerably between both closely and distantly related mammalian species.

As an example, three closely related primate species warrant mention. First, humans have kidneys with multiple pyramids and associated papillae are partly surrounded by funnel-shaped extensions of the pelvis termed calyces [35]. Humans may have seven to 13 minor calyces and two or three major calyces in each kidney. The result is a fairly complex collecting system that can be challenging to map and completely explore via endoscopy. Second, chimpanzees have kidneys with one elongated (and protruding) papilla and one calyx surrounding this papilla [38]. This type of renal pelvis would be fairly straightforward to visualize via endoscopy. Third, gorillas possess kidneys with a single fused papilla that terminates in a renal crest that also has a calyx partly surrounding it [38, 39]. A *renal crest* is a prominent ridge of tissue with a straight to

concave free edge that protrudes into the renal pelvis along a craniocaudal axis opposite to the outflow path of the ureter [23]. The renal crest is comprised of fused papillae of the renal pyramids and is covered by cuboidal rather than transitional epithelium[24]. Despite a somewhat similar overall organization of renal structure, these differences in pelvic anatomy would clearly look quite different when visualized with an endoscope advanced up the ureter.

Another variation in pelvic anatomy is presence of elaborate “leaf-like” projections, termed *fornices* and *secondary pouches*, that extend deep into the medulla in some species [40]. These projections of the renal pelvis are lined by thin epithelium, rather than transitional epithelium, and can dramatically increase the surface area of contact between the medulla and pelvic urine, perhaps favoring urea reabsorption. Similar to the variation in degree of pyramid fusion and extent of minor and major calyces in primates, the variation in presence and extent of these fornices and secondary pouches varies considerably within rodent species [40].

In the horse the renal pelvis is funnel-shaped, but flattened dorsoventrally. The inner medullary collecting ducts from the central part of the kidney of the horse open onto a renal crest to allow urine to exit into the pelvis via *ducts of Bellini*. In contrast, the collecting ducts from each pole of the kidneys do not open into the renal pelvis proper, but into two long tubes that have been called either the *terminal recesses* or *tubuli maximi* (singular, *tubulus maximus*), that extend from the renal pelvis toward the poles of the kidney [41].

Joseph Hyrtl, renowned Hungarian anatomist of the 19th century, is considered one of the pioneers in using corrosion casts to study mammalian anatomy [42]. Using this technique he produced anatomical descriptions and illustration of a number of cavitory anatomical structures including the renal pelvis of the horse. To the knowledge of this author, the first gross

description of the tubulus maximus was by Hyrtl in 1870 using the corrosion cast technique [43-45]. In 1898 His and Du Bois coined the term “*tubi maximi*” for these structures and characterized them as being flat (closed) in an empty state (post-mortem) [43-45]. They were also the first to report measurements as being few millimeters in width and about 4 cm in length into the caudal pole and about 7 cm in length into the cranial pole [41]. His and Du Bois speculated that the tubi maximi were a developmental adaptation and considered them large terminal collecting ducts draining urine from nephrons in the poles of the kidney to the renal pelvis [41].

Subsequent to these early reports, description of the terminal recesses or tubi maximi of the equine renal pelvis has been inconsistent in veterinary anatomy textbooks. Sisson describes the terminal recesses as gradually tapering extensions of the renal pelvis into the poles of the kidneys [14] while Nickel [27] actually has illustrations of “plastoid” casts of both equine renal pelves that demonstrate terminal recesses to have no tapering and a diameter similar to that of the proximal ureter. Descriptions in these textbooks would lead one to think that a small diameter flexible endoscope should allow complete visualization of the equine renal pelves with the ability to advance the endoscope to the ends of both recesses. Apparently, the early observations by Hyrtl [43] and His and Du Bois appear to have been overlooked and did not reach the English language veterinary anatomy textbooks. Mention of narrower tubi maximi in equidae is made by Maluf [45, 46] in several publications about comparative renal pelvic anatomy, but these all refer back to the original 1870 manuscript by Hyrtl.

For development of ureterorenoscopic diagnostic and therapeutic procedures in horses, it was essential to clarify these discrepancies in renal pelvic anatomy in prior publications. Consequently, the work described in this thesis was pursued to detail the anatomy of the renal

pelvis of the horse. A novel approach to the traditional use of corrosion casts to investigate cavitory anatomical structures was pursued; specifically, magnetic resonance imaging with three dimensional reconstruction was used to illustrate the cast material and structure of the renal pelvis, rather than corrosion of overlying renal parenchyma. Following this study, endoscopic and subgross and histological examination of the renal pelvis and collecting system was performed to definitively document equine renal pelvic anatomy.

BIBLIOGRAPHY

BIBLIOGRAPHY

1. Rassweiler, J., et al., The role of imaging and navigation for natural orifice transluminal endoscopic surgery. *J Endourol*, 2009. 23(5): p. 793-802.
2. Röcken, M., et al., Left- and right-sided laparoscopic-assisted nephrectomy in standing horses with unilateral renal disease. *Veterinary surgery : VS : the official journal of the American College of Veterinary Surgeons*, 2007. 36: p. 568-72.
3. Lansdowne, J.L., et al., Comparison of two laparoscopic treatments for experimentally induced abdominal adhesions in pony foals. *American journal of veterinary research*, 2004. 65: p. 681-6.
4. Voss, J.L. and B.W. Pickett, Diagnosis and treatment of haemospermia in the stallion. *J Reprod Fertil Suppl*, 1975(23): p. 151-4.
5. TRAUB, D. and C.M. Brown, *Equine endoscopy* 2nd Ed. 2 ed1997: Mosby, Inc.
6. Menzies-Gow, N., Diagnostic endoscopy of the urinary tract of the horse. In *Practice*, 2007. 29: p. 208.
7. Penninck, D., et al., Equine renal ultrasonography: normal and abnormal. *Veterinary Radiology & Ultrasound*, 1986. 27: p. 81-84.
8. Barratt-Boyes, S. and M. Spensley, Ultrasound localization and guidance for renal biopsy in the horse. *Veterinary Radiology & Ultrasound*, 1991. 32: p. 121-126.
9. Matthews, H.K. and R.L. Toal, A Review of Equine Renal Imaging Techniques. *Veterinary Radiology & Ultrasound*, 1996. 37: p. 163-173.
10. Pringle, J.K., N.G. Ducharme, and J.D. Baird, Ectopic ureter in the horse: Three cases and a review of the literature. *Can Vet J*, 1990. 31(1): p. 26-30.
11. Blikslager, A.T., et al., Excretory Urography and Ultrasonography in the Diagnosis of Bilateral Ectopic Ureters in a Foal. *Veterinary Radiology & Ultrasound*, 1992. 33: p. 41-47.
12. Shigemura, K., et al., Efficacy of combining flexible and rigid ureteroscopy for transurethral lithotripsy. *The Kobe journal of medical sciences*, 2010. 56: p. E24-8.
13. Somogyi, L., et al., Guidewires for use in GI endoscopy. *Gastrointestinal endoscopy*, 2007. 65: p. 571-6.

14. Holden, T., R.N. Pedro, and M. Monga, Accessory instrumentation in flexible ureteroscopy: Evidence-based recommendation. *Indian J Urol*, 2008. 24(4): p. 510-2.
15. Rubenstein, J.N., et al., Novel everting urologic access sheath: decreased axial forces during insertion. *J Endourol*, 2005. 19(10): p. 1216-20.
16. Kourambas, J., R.R. Byrne, and G.M. Preminger, Does a ureteral access sheath facilitate ureteroscopy? *J Urol*, 2001. 165(3): p. 789-93.
17. Rehman, J., et al., Characterization of intrapelvic pressure during ureteropyeloscopy with ureteral access sheaths. *Urology*, 2003. 61(4): p. 713-8.
18. Teichman, J.M., et al., Ureteroscopic management of ureteral calculi: electrohydraulic versus holmium:YAG lithotripsy. *J Urol*, 1997. 158(4): p. 1357-61.
19. L'Esperance J, O., et al., Effect of ureteral access sheath on stone-free rates in patients undergoing ureteroscopic management of renal calculi. *Urology*, 2005. 66(2): p. 252-5.
20. Zhang, J., et al., Cost-effectiveness analysis of ureteroscopic laser lithotripsy and shock wave lithotripsy in the management of ureteral calculi in eastern China. *Urol Int*, 2011. 86(4): p. 470-5.
21. Wang, D.W., J.Y. Wang, and X.M. Cao, [Compare the outcome of ureteroscopic lithotripsy with ureteroscopic management after failed extracorporeal shock wave lithotripsy for ureteral calculi]. *Zhonghua Wai Ke Za Zhi*, 2009. 47(4): p. 258-60.
22. Nakada, S.Y., et al., Long-term outcome of flexible ureterorenoscopy in the diagnosis and treatment of lateralizing essential hematuria. *The Journal of urology*, 1997. 157: p. 776-779.
23. Chauveau, A. and S. Arloing, *The comparative anatomy of the domesticated animals*. Search1873: D. Appleton and company.
24. Sisson S., G., *The Anatomy of the Domestic Animals*. 5th ed. Vol. 1. 1975, Philadelphia: W. B. Saunders.
25. Toribio, R.E., Essentials of equine renal and urinary tract physiology. *Vet Clin North Am Equine Pract*, 2007. 23(3): p. 533-61, v.
26. Yadava, R.P. and M.L. Calhoun, Comparative histology of the kidney of domestic animals. *American journal of veterinary research*, 1958. 19: p. 958-68.
27. Nickel, R., et al., *The viscera of the domestic mammals*. Annals of the ICRP/ICRP Publication. Vol. 23. 1973: Verlag Paul Parey. 173-196.

28. Parks, C.M. and M. Manohar, Distribution of blood flow during moderate and strenuous exercise in ponies (*Equus caballus*). *Am J Vet Res*, 1983. 44(10): p. 1861-6.
29. Kriz, W., Structural organization of the renal medulla: comparative and functional aspects. *Am J Physiol*, 1981. 241(1): p. R3-16.
30. Pallone, T.L., Z. Zhang, and K. Rhinehart, Physiology of the renal medullary microcirculation. *Am J Physiol Renal Physiol*, 2003. 284(2): p. F253-66.
31. Cowley, A.W., Jr., et al., The renal medulla and hypertension. *Hypertension*, 1995. 25(4 Pt 2): p. 663-73.
32. Pallone, T.L. and E.P. Sillardorff, Pericyte regulation of renal medullary blood flow. *Exp Nephrol*, 2001. 9(3): p. 165-70.
33. Park, F., et al., Evidence for the presence of smooth muscle alpha-actin within pericytes of the renal medulla. *The American journal of physiology*, 1997. 273(5 Pt 2): p. R1742-8.
34. Franchini, K.G. and A.W. Cowley, Jr., Renal cortical and medullary blood flow responses during water restriction: role of vasopressin. *Am J Physiol*, 1996. 270(6 Pt 2): p. R1257-64.
35. Dwyer, T.M. and B. Schmidt-Nielsen, The renal pelvis: machinery that concentrates urine in the papilla. *News Physiol Sci*, 2003. 18: p. 1-6.
36. Woollam, D., Casts of the ventricles of the brain. *Brain*, 1952. 75(2): p. 259-67.
37. Narath, P., *Renal Pelvis and Ureter* 1951, New York: Grune and Stratton.
38. Straus, W.L., *The Structure of the Primate Kidney*. *Journal of anatomy*, 1934. 69: p. 93-108.
39. Hosokawa, H. and T. Kamiya, Anatomical sketches of visceral organs of the mountain gorilla (*Gorilla gorilla beringei*). *Primates*, 1961. 3: p. 1-28.
40. Bankir, L. and C. de Rouffignac, Urinary concentrating ability: insights from comparative anatomy. *Am J Physiol*, 1985. 249(6 Pt 2): p. R643-66.
41. [41], E.H. and W. His, *Archiv für Anatomie und Entwicklungsgeschichte* 1898: Veit & Co.
42. Kyle, R.A. and M.A. Shampo, Joseph Hyrtl--anatomist of the 19th century. *Mayo Clin Proc*, 2001. 76(5): p. 456.
43. Hyrtl, J., *Das Nierenbecken der Säugethiere und des Menschen* 1870: Gerold.

44. Pfeiffer, E.W., Comparative anatomical observations of the mammalian renal pelvis and medulla. *Journal of anatomy*, 1968. 102: p. 321-31.
45. Maluf, N.S., Kidney of elephants. *The Anatomical record*, 1995. 242: p. 491-514.
46. Maluf, N.S., Anatomy of the kidneys of a newly born pigmy hippopotamus (*Choeropsis liberiensis* Morton). *Anat Histol Embryol*, 1978. 7(1): p. 28-48.

CHAPTER 2: ANATOMIC AND MORPHOLOGIC DESCRIPTION OF THE RENAL PELVIS OF THE HORSE USING MAGNETIC RESONANCE IMAGING OF POLYMER CASTS, URETEROPYELOSCOPY, AND HISTOLOGY

REASONS FOR PERFORMING STUDY: Descriptions of the equine renal pelvis in textbooks are inconsistent and unsuitable for guiding ureteropyeloscopy.

OBJECTIVE: To document the anatomy of the upper urinary collecting system, specifically the renal pelvis, of the horse.

METHODS: Kidneys were harvested from 10 horses. Magnetic resonance imaging was performed after distension of the renal pelvis with a polymer cast material. Transurethral ureteropyeloscopy of the upper urinary tract was performed in four horses and followed by histological and immunohistochemical examination of the renal medulla and pelvis.

RESULTS: The equine renal pelvis is a funnel-shaped cavity, flattened dorsoventrally in the craniocaudal direction. Multiple inner medullary collecting ducts (IMCDs) from the central part of the kidney open along an ~3 cm long renal crest that protrudes into the renal pelvis while IMCDs from each pole open into two long (6-7 cm), narrow *tubi maximi* that terminate at either end of the renal crest. The diameter of the distended *tubi maximi* are narrowest (~3 mm) at their junction with the renal crest. Openings of the *tubi maximi* could be visualized during ureteropyeloscopy in all horses and minor anatomical variation was observed. Histological examination confirmed entry of IMCDs along the lengths of the *tubi maximi* and the renal crest. Immunohistochemical staining for smooth muscle actin demonstrated increased amounts in a band pattern in the medullary region as well as at the junction of the *tubi maximi* with the renal crest.

CONCLUSIONS: Urine passes into the equine renal pelvis via IMCDs that terminate along the renal crest and along the course of the *tubi maximi*. Current endoscopic equipment can be used to visualize the renal pelvis and renal crest but cannot be advanced into the *tubi maximi*.

POTENTIAL RELEVANCE: The findings of this study will help guide future diagnostic and therapeutic ureteropyeloscopy.

INTRODUCTION

Urethroscopy and cystoscopy have been performed in horses since the 1970s to directly visualize the lower urinary tract (Voss and Pickett 1975; Sullins and Traub-Dargatz 1984; Traub-Dargatz and McKinnon 1988; Schott and Varner 1996; Menzies-Gow 2007). However, evaluation of the upper urinary tract has largely been accomplished using indirect imaging techniques including ultrasonography, intravenous and retrograde contrast pyelography, and nuclear scintigraphy (Schott *et al.* 1993; Tomlinson *et al.* 1993; Matthews and Toal 1996; Reef 1998).

In humans, endoscopic examination of the ureter and renal pelvis (ureteropyeloscopy) has become a routine procedure for direct visualization of the upper tract in patients with lithiasis, infection, neoplasia, and hematuria (Grasso and Bagley 1998; Rajamahanty and Grasso 2008; Geavlete *et al.* 2011). With reduction in diameter and increase in length of flexible endoscopes, ureteropyeloscopy is now possible in horses; however, knowledge of normal anatomy of the equine upper urinary tract, and variations thereof, is a prerequisite for accurate diagnostic interpretation.

Anatomy textbooks describe the equine renal pelvis as a funnel-shaped dilation of the upper ureter, flattened dorsoventrally along a craniocaudal axis [23]. Opposite the outflow path of the ureter is a prominent, slightly concave ridge of tissue termed the *renal crest* [23]. The renal crest is comprised of fused papillae, or apices of medullary pyramids, in the central portion of the kidney. Inner medullary collecting ducts (IMCDs) from this part of the kidney open onto the renal crest via papillary ducts allowing urine to exit into the pelvis. In addition, two diverticuli, referred to in textbooks as *terminal recesses* [23], extend from the pelvis towards each pole of the kidney. IMCDs from nephrons in the poles of the kidney open into these diverticuli. Illustrations of terminal recesses show them to be progressively tapering structures emanating from the renal pelvis [23]). Two textbooks (Sisson 1975; Nickel *et al.* 1979) also have illustrations of corrosion casts of the renal pelvis of both equine kidneys that depict terminal recesses that should be accessible by a small diameter endoscope and one source (Nickel *et al.* 1979) states that the terminal recesses are 6-10 cm in length with an average diameter of 5 mm. However, a more recently published textbook (Dyce *et al.* 2002) has a picture of a corrosion cast of the renal pelvis showing more narrow appearing terminal recesses, but the connection to the renal pelvis is not depicted. Similarly, a much earlier chapter by Cheivitz (1897), also based on examination of corrosion casts, describes the terminal recesses as narrow terminal collecting ducts for the poles of the kidney. Cheivitz (1897) and previous anatomists referred to in his chapter termed these structures *tubi maximi*. The *tubi maximi* were described to be a few mm in diameter and to be flat (closed) in the empty state. Clearly, if this earlier description is more accurate, as would be supported by the corrosion cast appearing in Dyce *et al.* (2002), the extent to which the collecting system of equine kidneys may be amenable to ureteropyeloscopic examination may be limited.

The purpose of this study was to investigate the anatomy and morphology of the upper urinary collecting system of the horse, specifically the renal pelvis. In addition to direct examination of corrosion casts of the renal pelvis, a novel method using magnetic resonance imaging (MRI) three-dimensional reconstruction of proximal ureteral and renal pelvic casts was employed to make measurements of the renal pelvis and terminal collecting system. Anatomy of the renal pelvis was also visualized directly via ureteropyeloscopy. Finally, subgross anatomical dissection, histology, and immunohistochemical labeling was performed to further describe the anatomy of the renal pelvis and inner medulla. In this report, the tubular extensions of the renal pelvis toward the kidney poles will be termed tubi maximi, rather than terminal recesses.

MATERIALS AND METHODS

Horses studied and specimens collected: 10 pairs of kidneys were harvested from horses, seven geldings and three mares with a mean age of 6 ± 3 (S.D.) yr, within 2 h of euthanasia. All horses had normal renal function and were subjected to euthanasia for reasons unrelated to this study. None of horses studied had been administered nephrotoxic medications within the prior 30 days or had any procedure performed that may have affected renal structure or function. Subsequently, ureteropyeloscopy was performed in four horses, two mares and two geldings with a mean age of 14 ± 9 yr with normal renal function, and immediately following endoscopy three of these horses (two geldings and one mare) were euthanized and their kidneys were removed for subgross anatomical dissection, histology, and immunohistochemistry. Both geldings were Thoroughbred racehorses that had been donated due to chronic lameness; thus, use of nonsteroidal anti-inflammatory drugs was likely in the past several months but neither had documented use of nephrotoxic medications within the preceding 2 weeks. The mare had been

treated with phenylbutazone (2.2. mg/kg, PO, q 12 h) for the previous 30 days for arthritis. The study protocol and all procedures performed were approved by the Animal Care and Use Committee of Michigan State University.

Measurements and polymer cast preparation: The 10 horses from which kidneys were harvested were weighed (± 2 kg) on a scale, scored for body condition (Henneke *et al.* 1983), and morphometric measurements were made: height at withers, length (point of shoulder to tuber ischii), and abdominal circumference. Subsequently, the kidneys and ~15 cm of the proximal ureter were removed, dissected free of fat and other connective tissue, and weighed (± 10 g) and volume of the tissues was determined by water displacement (± 5 ml). After review of photographs of all 10 sets of kidneys, renal length from the cranial pole to the middle section of the caudal pole was measured (± 1 mm) by drawing a line on the photographs (**Figure 1**). This measurement direction was selected because it was the most consistent axis for length measurement that was least affected by variation between specimens.

After volume determination, a rapidly setting silicone based polymer^a was infused into the ureter to fill the renal pelvis and proximal ureter. Polymer was infused until mild distension of the renal pelvis was visibly evident and moderate resistance to further injection was appreciated; the ureter was then ligated. The degree of pelvic distension and volume of polymer infused (35–40 ml in all specimens) was standardized after preliminary attempts revealed that infusion with a larger volume and greater force resulted in disruption of the pelvis and extension of cast material into the renal parenchyma. After allowing the polymer to harden for 15–20 min, T2-weighted magnetic resonance imaging (MRI)^b of both kidneys (0.2 mm slices) was performed with the

pair of kidneys resting on their ventral surfaces. Two- and three-dimensional images of each kidney and of the polymer within the renal pelvis were reconstructed using commercial software^c (**Figure 1 and 2**). Kidney length was measured along the same axis as in the photographs (**Figure 1**) and renal volume was measured after computer tracing and elimination of the cast material. Additional measurements obtained from three-dimensional reconstructions of the polymer casts included: diameter of the renal pelvis (craniocaudal direction at three locations), renal pelvis volume, renal crest length, length of the cranial and caudal tubi maximi, and diameter of the tubi maximi at three locations in a dorsal (or sagittal) plane (**Figure 2**). After completion of the MRI scans, kidneys were frozen for several days and after subsequent thawing renal parenchyma was gently dissected away from the polymer casts. The casts were then placed in a 1.0 N HNO₃ solution until the remaining renal parenchyma could be rinsed off to allow visual inspection of the casts.

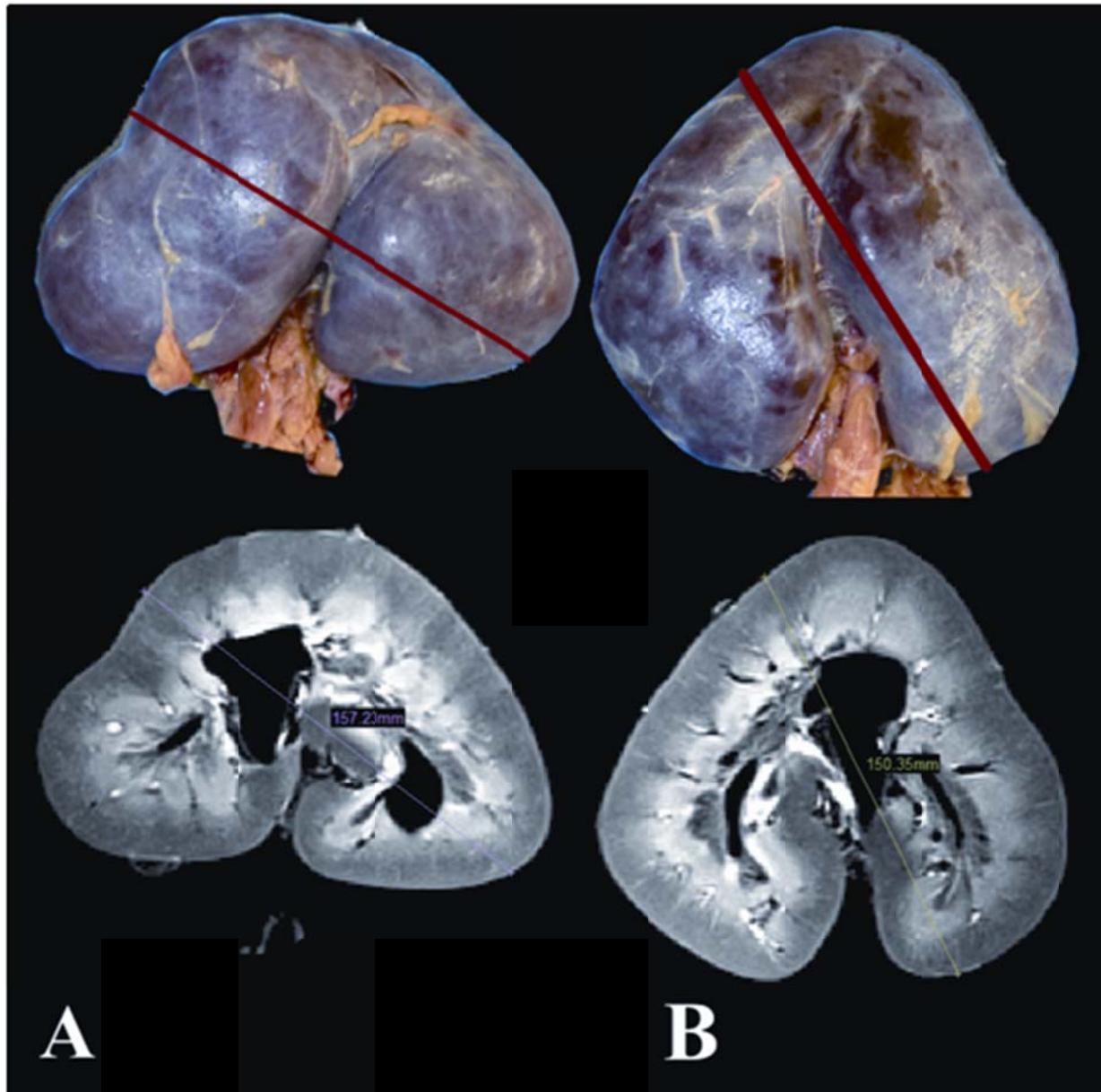


Figure 1: Dorsal plane photographs (top) and magnetic resonance images (bottom) of the left (A) and right (B) kidneys showing (lines) where kidney length was measured. “For interpretation of the references to color in this and all other figures, the reader is referred to the electronic version of this thesis”

Ureteropyeloscopy: Horses were restrained standing in stocks and sedated with detomidine hydrochloride^d (0.02 mg/kg, IV). An intravenous catheter was aseptically placed into the jugular vein. The tail was wrapped and pulled to the side and the perineum was prepared as for

cystoscopy (mares) or surgery (geldings). A urethral catheter was passed into the bladder of the geldings and a 7 cm vertical perineal urethrotomy (PU) was performed. In both sexes, 20 ml of a 2% lidocaine HCl solution were infused into the bladder through a bladder catheter for topical anesthesia after emptying the bladder of urine. The urethral sphincter was subsequently manually dilated until the index and middle fingers of a hand within a sterile glove could be easily passed into the bladder and the ureteral orifices could be palpated (Schott *et al.* 1990).

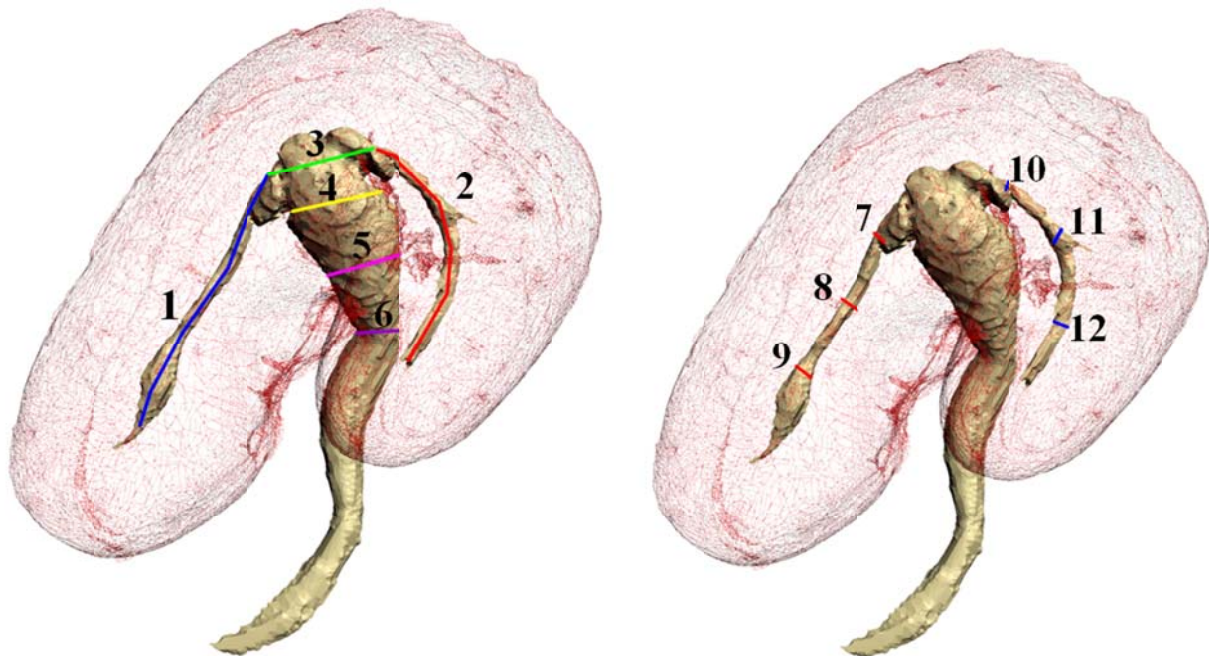


Figure 2: Three dimensional reconstruction of polymer within a left kidney detailing where measurements were made: 1. length of the cranial tubus maximus; 2. length of caudal tubus maximus; 3. renal crest length; 4. renal pelvis proximal diameter; 5. renal pelvis middle diameter; 6. renal pelvis distal diameter; 7. diameter of the pelvic end of the cranial tubus maximus 8. diameter of the midpoint of the cranial tubus maximus; 9. diameter of the pole end of the cranial tubus maximus; 10. diameter of the pelvic end of the caudal tubus maximus 11. diameter of the midpoint of the caudal tubus maximus; and 12. diameter of the pole end of the cranial tubus maximus.

The endoscope^e (110 cm working length, 4.9 mm outer diameter, 2.0 mm instrument channel, 120° field of view via angulation of 220°/120° [up/down]) was subsequently passed into the bladder via the urethra in mares or via the PU incision in geldings. Once the ureteral orifice was visualized, a flexible guide wire^f was passed through the instrument channel and directed into the ureteral opening and advanced ~10 cm. The index and middle fingers were used to grasp the end of the endoscope and manually guide it into the ureter. This procedure was easily accomplished in the two mares but was more challenging in the two geldings. Consequently, a 1 ml conical plastic pipette tip^g was passed over the guide wire and into the distal ureter to dilate the ureteral orifices in these animals (Schott *et al.*1990). Ureteral dilation allowed successful passage of the endoscope in three of four of the remaining ureters but one ureter was unable to be accessed in one gelding. Further, the PU incision was extended to ~10 cm and a partial dorsal sphincterectomy had to be performed in both geldings to allow adequate manual access to the ureteral orifices.

After the endoscope had been advanced ~10 cm into the ureter, the guide wire was removed and isotonic saline (0.9% NaCl solution) was infused (10 ml/min) with a fluid pump^h through the channel of the endoscope to maintain dilation of the ureter. The endoscope was then advanced without difficulty a further 50-60 cm to the renal pelvis which was fully explored. In three horses, phenol redⁱ was administered (1 mg/kg, IV) to further visualize urine excretion from papillary ducts along the renal crest and from the openings of the cranial and caudal tubi maximi.

After ureteropyeloscopy, three of the four horses were euthanized by IV administration of sodium pentobarbital (100 mg/kg, IV) for gross and histological examination of the kidneys.

Subgross anatomy, histology, and immunohistochemistry: Within 2 h of euthanasia harvested kidneys were infused with 60 ml of 10% formalin in a retrograde fashion through the ureter and the ureter was ligated, allowing the renal pelvis and *tubi maximi* to be fixed in a distended state. The kidneys were then fully submerged in 10% formalin. After 3 d of fixation, kidneys were sectioned (5-10 mm) along a sagittal axis (**Figure 3**) and each section was photographed. Subsections (0.5 cm thick x 2 cm long x 1.5 cm wide) of medulla, containing the *tubus maximus* and renal pelvis, were placed in tissue cassettes, sectioned at 4-5 μm , and stained with hematoxylin and eosin.

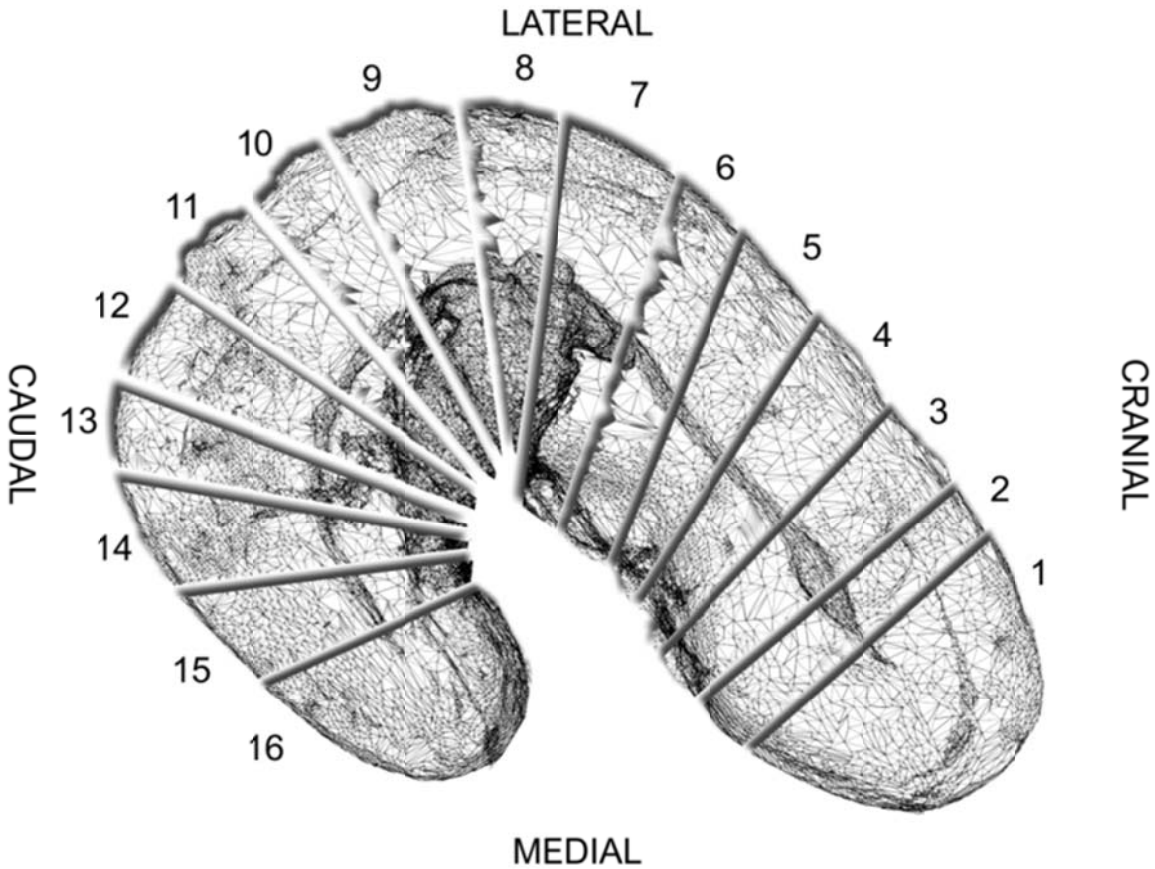


Figure 3: Diagram of a left kidney showing the pattern used to section the kidney for subgross anatomical and histopathological examination.

Additional 4-5 μm sections, adjacent to those examined by routine histology, were labeled with a murine monoclonal antibody against smooth muscle actin (αSMA). Sections were placed on slides coated with 2% 3-aminopropyltriethoxysilane and dried overnight at 56°C. Slides were deparaffinized in xylene and hydrated through descending grades of ethyl alcohol to distilled water. After placement in tris-buffered saline for 5 min to adjust to pH 7.4, heat-induced epitope retrieval was performed using 10 mM tris/1mM EDTA pH 9.0 buffer in a rice steamer for 30 min. Endogenous peroxidase was blocked utilizing a 3% hydrogen peroxide/methanol bath for 30 min followed by distilled water rinses. Standard avidin-biotin complex staining steps were subsequently performed at room temperature on a DAKO Autostainer^j. All staining steps were

followed by rinses in tris buffered saline and Tween 20^k. After incubation with normal goat serum^l for 30 min to limit non-specific protein binding, sections were incubated with avidin^m and biotinⁿ for 15 min. Primary antibody slides were incubated for 60 min with a murine monoclonal anti- α SMA antibody^o diluted 1:800 in Normal Antibody Diluent^p (NAD). After rinsing slides were subsequently incubated for 30 min with biotinylated caprine anti-murine IgG^q (11.0 μ g/ml in NAD) followed by incubation with RTU Vectastain Elite ABC Reagent^f for 30 min. Reaction development utilized Vector Nova Red peroxidase chromogen^s incubation for 15 min followed by counterstaining with Gill 2 hematoxylin^t for 15 sec.

Statistical analysis:

Data in this manuscript are presented as means \pm SD. Unpaired t-tests^u were performed to compare kidney weight, length, and volume between right and left kidneys and Pearson correlation analysis^u was used to compare renal measurements with body mass and other morphometric measurements. Bland-Altman assessment of agreement^u was subsequently performed to determine bias between direct measurements of length and volume with estimates obtained from software analysis of the MRI reconstructions. Unpaired t-tests or repeated measures analysis of variance^u were also performed to compare additional measurements made from the MRI reconstructions of renal pelvis casts.

RESULTS

Gross and MRI measurements: Kidney weights and measurements of kidney length and volume are presented in **Table 1**. The right kidney was heavier (by 20-200 g) than the left kidney in six horses while the left kidney was heavier (by 20-60 g) in the other four horses. Although mean weight of the right kidney was ~35 g heavier than that of the left kidney, there was not a significant difference between right and left kidney weights ($p=0.20$). There was a highly significant correlation between right and left kidney weights ($r=0.92$, $p<0.001$), but no significant correlations were found between individual or total kidney mass and body mass or other body morphometric measurements. Direct (necropsy) measurement of kidney length found the left kidney to be longer (by 0.5-2.9 cm) than the right kidney in seven horses while the right kidney was longer (by 0.1-1.0 cm) in the other three horses. The mean difference in length (left kidney 0.8 cm longer than the right kidney) approached significance ($p=0.06$). Highly significant correlations were found between right and left kidney lengths ($r=0.78$, $p<0.01$) and between right kidney mass and right kidney length ($r=0.80$, $p<0.01$) but there was no correlation between left kidney mass and left kidney length ($r=0.41$, $p=0.24$). Further, there were no significant correlations between kidney lengths and body mass or other body morphometric measurements.

Measurement of kidney volume by water displacement found the right kidney to be larger (by 40-180 cm³) than the left kidney in seven horses while the left kidney was larger (by 10-20 cm³) in the other three horses. The mean difference in volume (right kidney ~70 mm³ larger than the left kidney) was a significant finding ($p<0.02$). Highly significant correlations were found between right and left kidney volumes ($r=0.91$, $p<0.01$). Further, highly significant correlations were also found between kidney volume and kidney weight and length for each kidney (r values

0.64 or greater) but again there were no significant correlations between kidney volumes and body mass or other body morphometric measurements.

Table 1: Mean ± S.D. values (range) for kidney weight, kidney length measured at necropsy, kidney length measured via MRI, kidney volume measured by water displacement, and kidney volume measured by MRI in 10 horses.

Measurement	Left kidney	Right kidney
Mass (g)	960 ± 130 (760-1200)	990 ± 180 (740-1400)
Length (necropsy, cm)	18.0 ± 1.8 (15.5-21.0)	17.2 ± 1.5 (15.0-18.1)
Length (MRI, cm)	18.1 ± 1.8 (15.6-20.4)	17.3 ± 1.6 (14.7-19.3)*
Volume (water displacement, cm ³)	810 ± 140 (610-1060)	880 ± 180 (600-1240)*
Volume (MRI, cm ³)	820 ± 160 (610-1090)	890 ± 180 (620-1250)*

* denotes values that are significantly different (p<0.05) between kidneys

Measurements of kidney length and volume made from MRI reconstructions were not different than necropsy measurements; however, left kidney length was greater (p<0.05) than right kidney length with this measurement method. Further, Bland-Altman analysis comparing kidney length measurement methods yielded a bias ± 0.95% limit of agreement of -0.9 ± 5.1 cm for the left kidney and -0.6 ± 6.2 cm for the right kidney. Similarly, Bland-Altman analysis comparing kidney volume measurement methods yielded a bias ± 0.95% limit of agreement of -10 ± 62 cm³ for the left kidney and 9 ± 35 cm³ for the right kidney. For both kidney length and volume, bias was less than 5% of the actual measurement using either method. This level of agreement supported use of MRI measurements for remaining parameters including renal crest length, renal pelvic volume and diameters, and length and diameter of the *tubi maximi* (Table 2).

Renal crest length and renal pelvis volume were not different between the right and left kidneys. Not surprisingly, the diameter of the renal pelvis narrowed from the renal crest to the proximal ureter (distal renal pelvic diameter measurement) in both kidneys but measurements were not different between kidneys. The length of the cranial and caudal *tubus maximus* varied considerably (by 3-6 cm) in both kidneys but significant differences were not detected, either between cranial and caudal lengths or between kidneys. A highly significant correlation ($r=0.72$, $p<0.01$) was found between kidney length and cranial *tubus maximus* length but there was no association between kidney length and caudal *tubus maximus* length. The diameter of the *tubi maximi* narrowed from their origin in the poles of the kidneys to their termination at the renal pelvis in all but the caudal *tubus maximus* of the left kidney ($p=0.08$). In fact, the narrowing of the *tubus maximus* at its junction with the renal pelvis could be well appreciated by gross inspection of the corrosion casts (**Figure 4**).

Ureteropyeloscopy: The endoscope was successfully passed to the level of renal pelvis in seven of eight kidneys attempted. The left kidney of one of the geldings could not be examined due to an inability to pass the endoscope into the left ureter despite repeated dilation of the ureteral orifice. In general, the urethra and ureteral orifices were more readily accessible through the vestibule of the mare than through a perineal urethrotomy incision in geldings.

Once the endoscope was successfully passed into the ureter, ureteropyeloscopy was a straightforward procedure. The ureteral epithelium is pale yellow and arranged in prominent longitudinal folds and peristalsis can be observed. As the endoscope was advanced into the renal pelvis the cranial portion of the renal crest is initially observed and the endoscope tip has to be

manipulated caudally to visualize the entire renal crest and openings of the tubi maximi (**Figures 5A&B**). Presence of air bubbles facilitates dorsal orientation and the cranial portion of the renal pelvis is to the right when examining the left kidney and to the left when examining the right kidney.

Table 2: Mean \pm SD values (range) for MRI measurements of renal crest length, renal crest volume, diameter of the renal pelvis, length of the cranial and caudal tubi maximi, and diameter of the cranial and caudal tubi maximi at their origin (pole end), midpoint, and termination (pelvis end) in 10 horses.

	Renal crest length (mm)		Renal crest volume (cm ³)			
Left kidney	29.8 \pm 6.2 (23.3-43.3)		31.6 \pm 10.3 (20.6-58.2)			
Right kidney	30.1 \pm 5.4 (22.7-40.7)		34.2 \pm 10.3 (22.4-59.9)			
	Renal pelvis diameter (mm)					
	proximal (measure 4)	middle (measure 5)		distal (measure 6)		
Left kidney	21.4 \pm 6.0 (12.6-31.5) ^a	17.0 \pm 4.7 (11.6-27.8) ^b		13.0 \pm 2.1 (8.3-15.6) ^b		
Right kidney	20.8 \pm 4.9 (15.7-33.1) ^a	17.7 \pm 4.4 (13.0-27.9) ^{ab}		14.6 \pm 2.7 (10.0-19.6) ^b		
	Cranial <i>tubus maximus</i> length (MRI, cm)			Caudal <i>tubus maximus</i> length (MRI, cm)		
Left kidney	7.0 \pm 1.6 (5.1-9.3)			6.4 \pm 1.2 (4.9-8.6)		
Right kidney	6.8 \pm 1.0 (4.8-7.9)			7.5 \pm 1.8 (5.0-10.9)		
	Cranial <i>tubus maximus</i> diameter (mm)			Caudal <i>tubus maximus</i> diameter (mm)		
	pelvis end (measure 7)	midpoint (measure 8)	pole end (measure 9)	pelvis end (measure 10)	midpoint (measure 11)	pole end (measure 12)
Left kidney	3.1 \pm 1.0 ^a (1.9-4.7)	4.8 \pm 1.6 ^b (3.0-8.7)	5.2 \pm 2.3 ^b (2.1-9.6)	3.2 \pm 1.0 (1.7-4.9)	3.7 \pm 1.3 (1.2-5.7)	4.5 \pm 1.5 (2.0-7.1)
Right kidney	3.6 \pm 1.3 ^a (2.3-5.9)	4.7 \pm 1.2 ^{ab} (3.3-7.5)	5.6 \pm 1.5 ^b (3.0-7.6)	2.6 \pm 0.8 ^a (1.3-3.7)	3.8 \pm 1.0 ^b (3.0-6.2)	5.2 \pm 2.1 ^b (2.3-8.8)

^a different superscript letters within a row denote values that are significantly different (p<0.05)

Capillaries, often tortuous in nature, are apparent along the length of the renal crest and fornices that can only be partly explored are present above and below the prominent renal crest (**Figure**

5B) Further, anatomic variation was found in the openings of the tubi maximi (variation in depression of the openings of the tubi maximi, **Figures 5B&C**) as well as along the renal crest (a recessed area in the center of the renal crest was found in one kidney, **(Figure 5C)**). Within 5 min after IV administration of phenol red, red-discolored urine could be seen exiting both tubi maximi (**Figures 5D&E**) as well as from individual papillary ducts along the central portion of the renal crest (**Figure 5F**). Excretion of phenol red colored urine from the tubi maximi and individual papillary ducts along the renal pelvis appeared somewhat coordinated and pulsatile in nature; however, this observation may have been an artifact of the infusion of saline through the instrument channel of the endoscope.

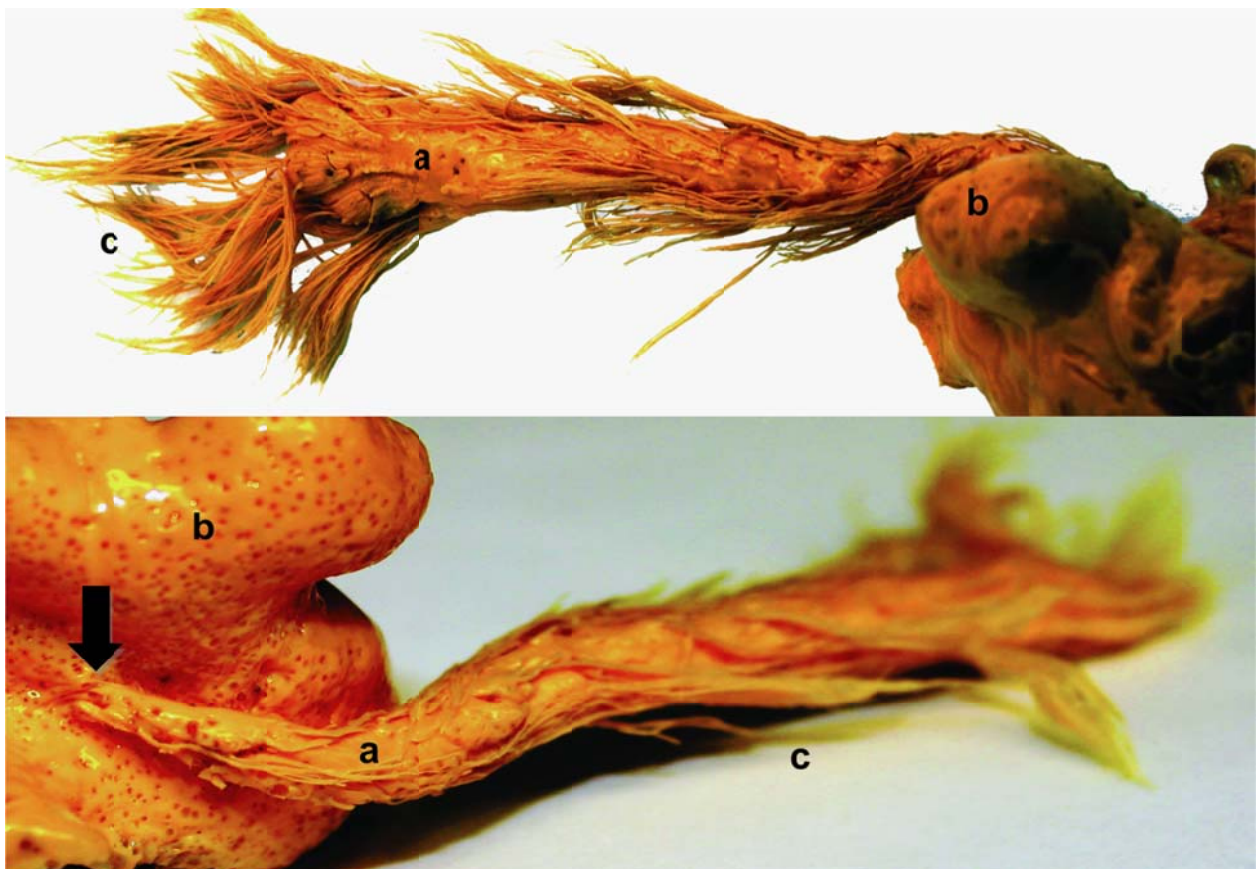


Figure 4: Corrosion polymer cast of the renal pelvis: top panel shows a tubus maximus (a) extending from the renal pelvis (b) with polymer extending into numerous papillary ducts (c) along its length; bottom panel shows the narrowing of the tubus maximus at its junction with the renal pelvis (arrow)

Subgross anatomy, histology, and immunohistochemistry: Subgross dissection of kidneys fixed by distension of the renal pelvis with 10% formalin clearly shows that the ureter dilates as it enters the renal hilum to form the funnel-shaped renal pelvis. The pelvis is flattened dorsoventrally and extends into fornices above and below the renal crest. The renal crest protrudes into the pelvis and is a slightly concave structure that appears to follow the curvature of the kidney. The renal pelvis of the horse was limited to the hilum of the kidney and did not extend into calyces. Subgross dissection of kidneys fixed by distension clearly revealed distended tubi maximi, similar in appearance as determined by MRI reconstruction, extending from the renal crest towards both kidney poles (**Figure 6**). Histologic examination revealed that the tubi maximi were lined with transitional uroepithelium similar to that covering the renal crest (**Figure 7**). Surrounding the tubus maximus, numerous smaller diameter inner medullary collecting ducts (IMCDs) appeared to run in a parallel direction with the tubus maximus (**Figure 7A&B**) but inspection of the corrosion casts (**Figure 4**) confirms that the IMCDs connect with the tubus maximus. Immunohistochemical labeling for α SMA revealed patchy areas of immunostaining adjacent to most uroepithelial surfaces (**Figure 7M-P**) but the most intense areas of immunolabeling were in the outer part of the inner medulla (**Figure 7E&F**) as well as around the tubi maximi, especially where it entered the renal pelvis along the renal crest (**Figure 7G and Figure 8**). Intense α SMA immunolabeling was also detected surrounding the papillary ducts where they terminated on the renal crest (**Figure 7H**).

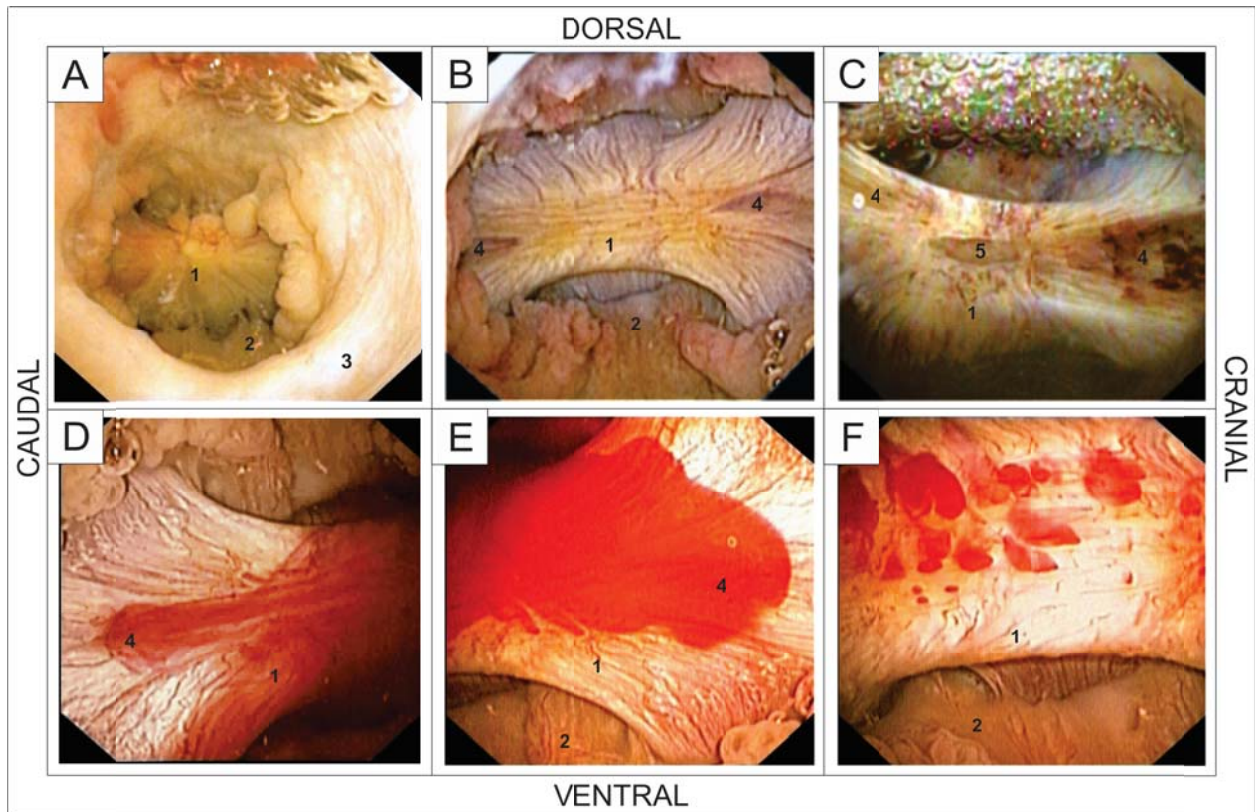


Figure 5: Ureteropyeloscopic images of the renal pelvis before (A-C) and after (D-F) intravenous administration of phenol red (orientation - cranial to the left, bubbles are dorsal): A. appearance of the renal crest (1) surrounded by uroepithelium (2) at the proximal aspect of the ureter (3); B. closer view of the entire renal crest within the renal pelvis showing fornices (2) above and below the renal crest and openings of the tubi maximi (4) towards either end of the renal crest; C. anatomic variation of the renal pelvis with a recess in the center (5) into which several papillary ducts open; D. cranial aspect of the renal crest showing urine discolored by phenol red entering the renal pelvis from the cranial tubus maximus (4); E. caudal aspect of the renal crest showing urine discolored by phenol red entering the renal pelvis from the caudal tubus maximus (4); and F. central portion of the renal crest showing urine discolored by phenol red exiting numerous papillary ducts.

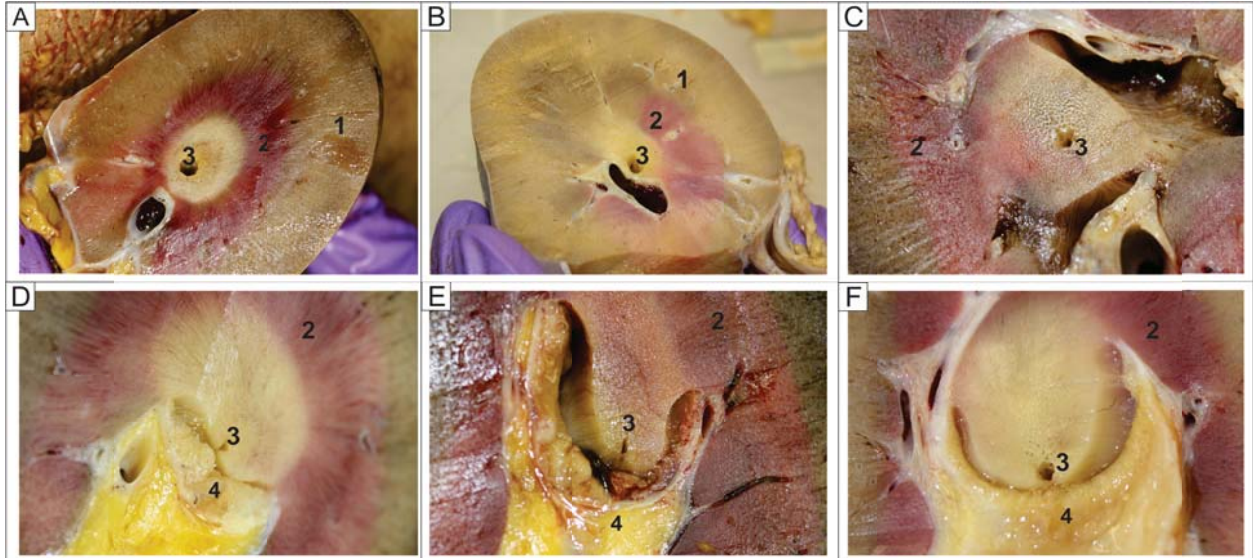


Figure 6: Panels A-C: pictures of subgross sagittal sections of a left kidney (fixed by distension of the renal pelvis with 10% formalin) showing the cortex (1), outer medulla (2), and inner medulla and tubus maximus (3) at the cranial pole end (A, section 2, see Figure 3 for section locations), the midpoint (B, section 4), and near the pelvis (C, section 6); panels D-F: pictures of subgross sagittal sections (section 6 or 10) of kidneys of three horses near the junction of the tubus maximus with the renal pelvis, also showing uroepithelium at the origin of the ureter.

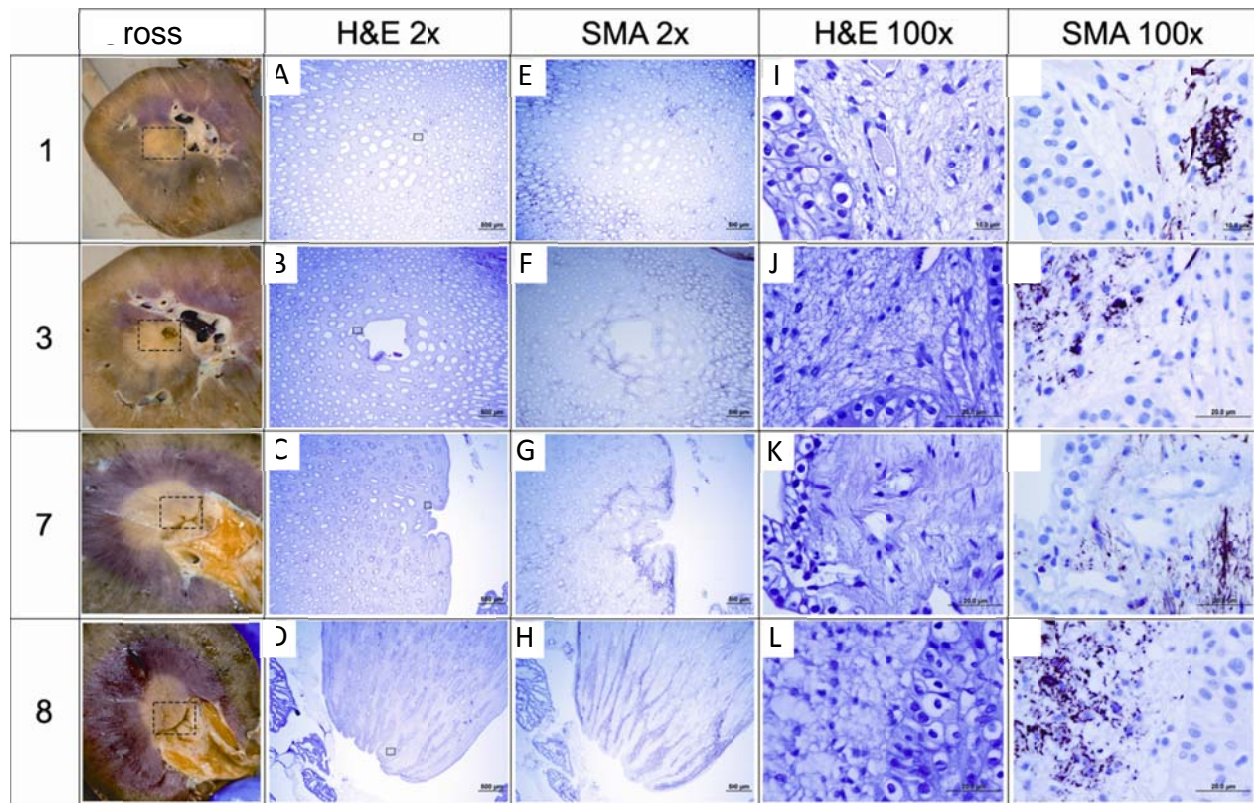


Figure 7: Subgross anatomic photographs (column 2) and low (2x, columns 3 & 4) and high power (100x, columns 5 & 6) photomicrographs stained with hematoxylin and eosin (columns 3 & 5) and immunolabeled for smooth muscle actin (SMA, columns 4 & 6). The numbers in column 1 refer to the kidney sections illustrated in Figure 3 and the small dashed-lined boxes in columns 2 & 3 show the areas enlarged in columns 3 & 4 and 5 & 6, respectively. Note the more intense SMA immunolabeling towards the periphery in panel E and the upper right of panel F as well as surrounding the mid-portion of the tubus maximus (panel F) and, even more intensely, around the tubus maximus as it enters the renal pelvis (panel G). Intense SMA immunolabeling was also detected surrounding the papillary ducts as they terminated on the renal crest (panel H). The higher magnification photomicrographs reveal patchy SMA immunolabeling in the connective tissue adjacent to most uroepithelial surfaces.

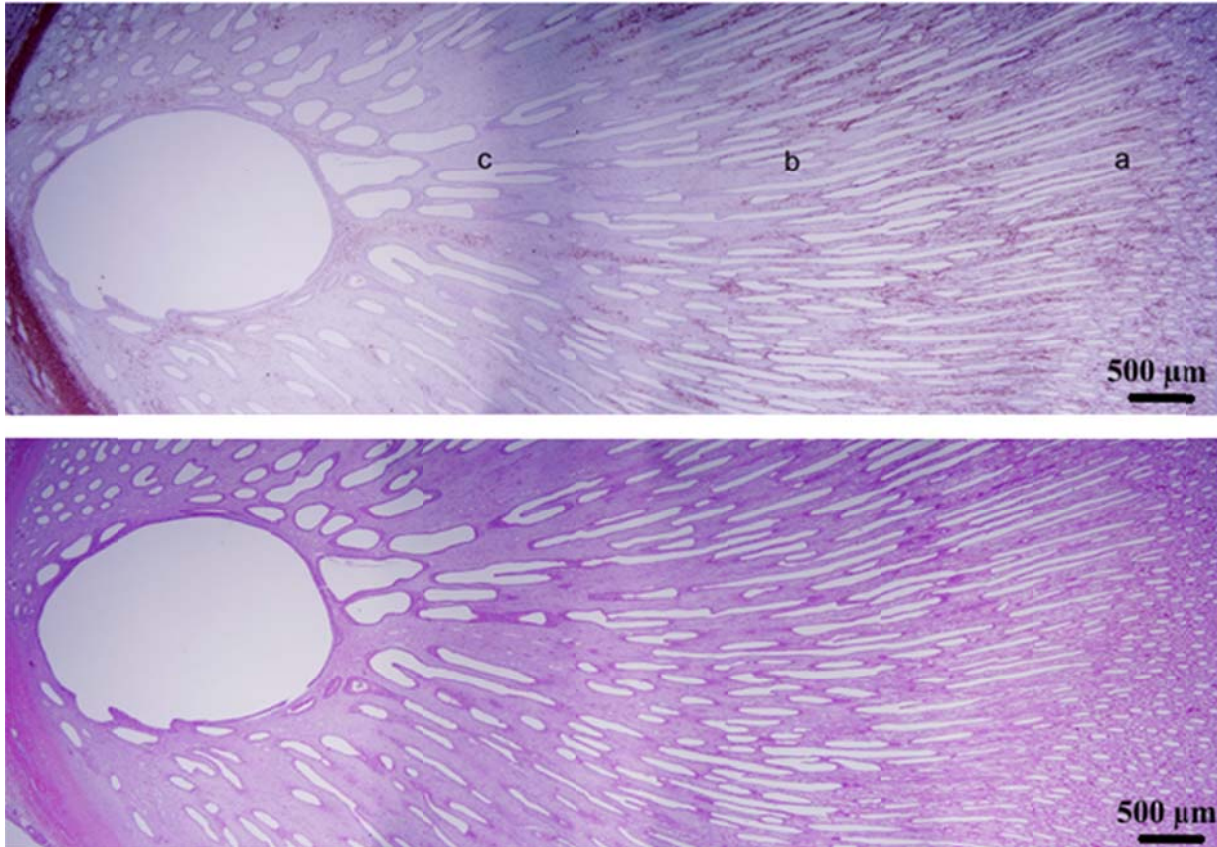


Figure 8: Photomicrographs of a sagittal section (section 4 in Figure 3) stained with hematoxylin and eosin (lower panel) and for smooth muscle actin (SMA, upper panel). Note the more intense aggregates of SMA immunolabeling in the outer portion of the inner medulla (between a and b), along a column extending into the deepest portion of the medulla (below c), as well as around the tubus maximus (the more diffuse dark band running from top to bottom to the right of c is an artifact).

DISCUSSION

It should be emphasized that the impetus for this work was to advance clinical application of endoscopy to diagnostic evaluation and therapeutic intervention in upper urinary disorders in horses. However, before ureteropyeloscopy could be developed into a clinical tool, basic knowledge of endoscopic anatomy of the normal renal pelvis was needed. To this end, we started by reviewing current and past anatomy textbooks and found variation in descriptions of the collecting system of the renal pelvis (see Introduction). Specifically, the extensions of the renal pelvis into the poles of the kidneys were described as either progressively tapering terminal recesses or more narrow tubules termed *tubi maximi*. A small diameter endoscope would more likely be able to be passed into the former as compared to the latter. Next, anatomists studied renal specimens that were no longer perfused with blood and producing urine; consequently, the collecting system was collapsed. Although several authors produced corrosion casts to better examine the renal pelvis as it would have appeared *in vivo*, casts were also variable in appearance and poorly reproduced as illustrations in the era before high resolution digital photography became available. Our findings clearly document that the renal pelvis of the horse consists of a large central compartment into which urine from the mid-portion of the kidney empties via numerous papillary ducts exiting on the renal crest. Further, the most distal collecting system of the poles of the kidneys consist of a tubular structure (5-10 cm in length and 3-5 mm diameter) into which many IMCDs from these parts of the kidney empty. Both our corrosion casts and MRI reconstructions document that these tubular structures become most narrow as they join the renal pelvis proper. Consequently, we prefer the early term *tubus maximus* as the most appropriate descriptor for this innermost collecting tubule of the poles of equine kidneys. Although currently available endoscopic equipment can be passed via the

bladder and ureter into the renal pelvis of the horse, the narrow diameter of the openings of the tubi maximi into the renal pelvis precludes full ureteropyeloscopy of the equine kidney at this time.

Comparisons to other species

Although the subgross and histologic structure of the renal cortex and medulla has been well studied in many species, less attention has been focused on variations in morphology of the renal pelvis. Eloquently, in 1951 Naranth stated “hardly any organ in the Mammalia exhibits such variations in form as the renal pelvis” [37]. Of further interest, there do not appear to be discernible taxonomic patterns of renal pelvis morphology along family lines. As mammals evolved greater in size, the kidneys of some species underwent increased length of the pelvic crest (e. g., camels and giraffes) while the collecting system of other species formed calyces, extensive fornices or recesses, or tubi maximi. Development of fornices or recesses and secondary pouches has been described in several groups of mammals, including carnivores, ruminants, and rodents. These fornices or recesses consist of “leaf-like” invaginations of the pelvis that project laterally into the outer zone of the medulla, breaking it into distinct segments surrounded by pelvic urine on three sides” [40].

The Perissodactyla are an order of large hoofed mammals that have kidneys with tubi maximi. They are represented by the *Equidae*, *Rhinocerotidae*, and *Tapiridae* [27, 43, 47]. Our work has confirmed the existence of *tubi maximi* in the horse, structures that are larger diameter collecting ducts originating at each end of the renal crest and extending along the coronal axis of the kidney towards the cranial and caudal poles. The openings of the tubi maximi into the renal pelvis were

also found to be narrowest portion of these tubular structures. The physiological significance of this finding as well as detection of more intense immunostaining against SMA around the tubi maximi, especially at their openings into the renal pelvis remains unclear but could suggest a contractile function of the tubi maximi with a sphincter like opening into the renal pelvis. Documentation of a contractile and sphincter function would require further investigation but could support that the inner medullary collecting system is not simply a passive tube but an active tissue that both “squeezes” urine into the renal pelvis and limits potential retrograde flow.

CONCLUSION

Current and older anatomy textbooks had variation in descriptions of the collecting system of the renal pelvis of the horse especially with regard to the extensions of the renal pelvis into the poles of the kidneys. Tubular extensions of the renal pelvis into both kidney poles have been described as either progressively tapering terminal recesses or more narrow tubules termed tubi maximi. Varying dissection and examination techniques (e.g., using renal specimens that were no longer perfused with blood in which the collecting system was collapsed as compared to studying corrosion casts of the renal pelvis) used by anatomists to produce these textbook description likely explain the reported discrepancies. The work detailed in this thesis clearly documents that the renal pelvis of the horse consists of a large central compartment into which urine from the mid-portion of the kidney empties via numerous papillary ducts exiting on the renal crest. Further, the most distal collecting system in the poles of the kidneys consist of a tubular structure (5-10 cm in length and 3-5 mm diameter) into which many IMCDs from the poles of the kidneys empty. Both the corrosion casts and MRI reconstructions documented that these tubular structures become most narrow as they join the renal pelvis proper. Consequently, the early term tubus maximus appears to be the most appropriate descriptor for this innermost collecting tubule of the poles of equine kidneys. Unfortunately, currently available endoscopic equipment only allows examination of the ureter and renal pelvis proper of upper urinary tract of the horse at this time.

BIBLIOGRAPHY

BIBLIOGRAPHY

- Dyce, K.M., Sack, W.O. and Wensing C.J.G. (2002) The Abdomen of the Horse. In: *Textbook of Veterinary Anatomy*, 3rd edn., Saunders, Philadelphia. pp. 525-544.
- Geavlete, P., Multescu, R. and Geavlete, B. (2011) Retrograde flexible ureteroscopy: reshaping the upper urinary tract endourology. *Arch. Esp. Urol.* 63, 3-13.
- GRASSO, M. AND BAGLEY, D. (1998) SMALL DIAMETER, ACTIVELY DEFLECTABLE, FLEXIBLE URETEROPYELOSOPY. *J. UROL.* 160, 1648-1653.
- König, H.E., Maierl, J. and Liebich, H.-G. (2007) Urinary System. In: *Veterinary Anatomy of Domestic Animals*, 3rd edn., Eds: H.E. König and H.-G. Liebich, Schattauer, Stuttgart. pp 391-405.
- Matthews, H.K. and Toal, R.L. (1996) A review of equine renal imaging techniques. *Vet. Radiol. Ultrasound* 37:163-173.
- Menzies-Gow, N. (2007) Diagnostic endoscopy of the urinary tract of the horse. In *Pract.* 29, 208-213.
- Schummer, A., Nickel, R. and Sack, W.O. (1979) Urogenital System. In: *R. Nickel, A. Schummer, E. Seiferle The Viscera of the Domestic Mammals*, 2nd edn., Springer-Verlag, New York. pp 282-304.
- Rajamahanty, S. and Grasso, M. (2008) Flexible ureteroscopy update: indications, instrumentation and technical advances. *Indian J. Urol.* 24, 532-537.
- Reef, V.B.: *Equine Diagnostic Ultrasound*. WB Saunders, Philadelphia, 1998
- Schott, H.C., Roberts, G.D., Hines, M.T. and Byrne, B.A. (1993) Nuclear scintigraphy as a diagnostic aid in the evaluation of renal disease in horses. *Proc. Am. Ass. equine Practnrs.* 39, 251-254.
- Schott, H.C. and Varner, D.D. (1997) Urinary Tract. In: *Equine Endoscopy*. 2nd edn., Eds: J.L. Traub-Dargatz and C.M. Brown, Mosby, St. Louis. pp 238-259.
- Shively, M.J. (1984) Urinary System. In: *Veterinary Anatomy, Basic, Comparative, and Clinical*. Texas A & M University Press, College Station. pp 325-338.
- Sisson S. (1975) Equine Urogenital System. In: *Sisson and Grossman's The Anatomy of Domestic Animals*, Vol 1, 5th edn., Ed: R. Getty, W.B. Saunders, Philadelphia. pp 524-549.

- Sullins, K.E. and Traub-Dargatz, J.L. (1984) Endoscopic anatomy of the equine urinary tract. *Comp. cont. educ. pract. vet.* 11, S663-S668.
- Traub-Dargatz, J.L. and McKinnon, A.O. (1988) Adjunctive methods of examination of the urogenital tract. *Vet. Clin. N. Am.: Equine Pract.* 4, 339-358.
- Voss, J.L. and Pickett, B.W. (1975) Diagnosis and treatment of haemospermia in the stallion. *J. Reprod. Fertil. Suppl.* 23, 151-154.